Artwork imaging from 370 nm to 1630 nm using a novel multispectral system based on LEDs

Jorge Herrera-Ramirez[1], Meritxell Vilaseca[1], Francisco J. Burgos[1], Lídia Font[2], Rosa Senserrich[3], Jaume Pujol[1]

[1] *Centre for Sensors, Instruments and Systems Development (CD6), Universitat Politècnica de Catalunya (UPC), Terrassa, Barcelona, Spain.*
[2] *History Museum of the City of Barcelona (MUHBA), Barcelona, Spain.*
[3] *College of Fine Arts, University of Barcelona, Barcelona, Spain.*

ABSTRACT

Although multispectral systems are relatively new to the cultural heritage studies, their use as a non-contact method for analysis of artworks has shown promising results. In this work we report on the application of a novel portable multispectral system based on Light-Emitting Diodes (LED) for artwork imaging. This system provides spectral information in a wide spectral range from 370nm to 1630nm with a field of view (FOV) of 25x25cm^2 by using two different image sensors in synchrony with 23 bands of illumination. The spectral information for each point is estimated and validated via two methods of spectral estimation and three different metrics of evaluation. The system is utilized to the study of masterpieces of Catalonian art, showing the potential of a cost effective and versatile system not only in reconstructing color information, but also revealing features not identified before.

INTRODUCTION

Spectral imaging technology has been in process of development since around 4 decades ago. More specific names have been given to describe the spectral imaging technology attending to the increase in the number of used spectral bands and the reduction of spacing between them. This has led to the appearance of terms like multispectral, hyperspectral or ultraspectral imaging [1]. Certainly, the rapid development of semi-conductors and the technologies related have had great influence in the variety of applications where the spectral imaging can be found today. Initially, this technology was mainly restricted to astrophysics, remote sensing and terrestrial military applications [2], but nowadays it is present in other fields of research including medicine, biometrics, environmental sciences, pharmacology, food engineering and agriculture [3–7].

In the recent years, spectral image acquisition has gained popularity in the community dealing with cultural heritage applications for several reasons [8]. One of them is that accessing to the spectral reflectance gives more accurate color reproduction, avoiding the dependence on the illumination and the acquisition devices [9]. Thus, institutions can carry out processes of digital archiving and reproduction of their collections [10]. Other important consideration of using spectral imaging in this field is that the obtained information is objective, repeatable and do not suffer from aging, and hence, it allows monitoring the status of conservation of the

artworks. A third advantage is that spectral imaging permits material identification. Furthermore, data from nonvisible spectral ranges can provide important information. Infrared (IR) reflectography or ultraviolet (UV) luminiscence can give insight into the history of the artwork, the artist's methods or serve as a tool of conservation status diagnosis. Also, spectral features of the materials can be drawn from these nonvisible parts of the spectrum [11,12]. Some of these tasks have been performed using other tools, for example for the identification of materials several analytical chemical techniques have been developed. Some of these techniques require the extraction of a small sample (scanning electron microscopy, chromatography, and polarization microscopy). Other techniques can be employed in situ, such as X-ray fluorescence spectroscopy, Raman spectroscopy or Fiber Optic Reflectance Spectroscopy (FORS). But all of them are point measurement techniques that are used over a selection of points, usually determined by visual inspection. Some of these techniques such as FORS can be devised to generate a scanning over the complete surface of the painting, but it entails long times of acquisition making it impractical in almost all cases. In situ spectral imaging systems can provide entire paint acquisition, and depending on the specific implementation, at least can guide the site selection for further study with point measurement methods.

Different approaches for multispectral imaging systems have been implemented. The main types are single point spectrometers with 2-D scanning systems[13], digital cameras combined with linescan or pushbroom spectrographs [5], color filter wheels [14], filter mosaics [15], lenslet arrays together with narrowband filters [16,17] , and tunable filters of liquid crystal or acousto optic technology [18,19]. Each of these approaches has its compromises among operational speed, spectral and spatial resolutions, and costs. These systems regularly use a light source with wide spectral range of emission, such as a halogen or mercury-xenon lamp. In this sense, a different approach is offered by the current development of the light-emitting diode (LED) technology. This technology has got improvements in several aspects: wavelengths availability, efficiency, emission power, life cycle, and it is still in constant evolution. The LED elements offer narrow spectral emissions in wavelengths from the UV to the IR spectral ranges. They allow illuminating with specific wavelengths or customized combinations of them in a fast way and in a switching synchrony with the imaging sensors. They can also be combined with filters either to control the spectral emission of the LEDs or to evaluate luminescence [20]. Under these circumstances, some proposals of multispectral systems using LED illumination and covering the visible range of the electromagnetic spectrum have been published in the last few years [3,20–23]. These systems have been used in different applications such as in measurements of cortical oxygenation [20], in microspectroscopic measurements in molecular multiplex assays [22] or ocular fundus imaging [3].

In the field of artwork imaging the employment of multispectral systems using LED illumination have the advantage of limiting the exposure of the target surface to light, which may be desirable for conservation purposes [24]. This approach might provide low acquisition times through fast switching and possibility of illumination of extended areas, and represents a compact approach to assemble illumination and acquisition in the system without mobile parts, which can be reliably operated in situ.

In this account, we report on the use of a LED based multispectral system for imaging of paintings. The system covers a wide spectral range from 370nm to 1630nm that has been shown to provide relevant information. We describe the system setup in the following section, and provide a brief description of the methods used for spectral reconstruction as well as the metrics for performance evaluation. Some applications to the study of Catalan masterpieces are finally reported with the aim of showing the potential of the system in this field.

METHODS AND MATERIAL

SYSTEM SETUP

In order to acquire spectral images in the proposed spectral range, the imaging equipment featured two main parts or modules, each one comprising an imaging sensor and a spectral light source based on LEDs. These two parts can be associated to its own spectral window, the first one covering from 370nm to 950nm and the second one from 930nm to 1630nm. The first part (module 1) consists of a cooled CCD monochrome camera (QICAM Fast 1394, Qimaging, Canada) with 12 bit depth of digitalization and a sensing area of 1392 x 1040 pixels. We removed the near IR filter of this camera in order to have spectral response till 950 nm. This camera is coupled to a lens (Cinegon Serie Compact 12 mm f/# 1.4, Scheider-Kreuznach, Germany) with high transmittance between 400 nm and 1000 nm. The correspondent spectral light source has 16 channels given by different groups of LEDs (peak wavelengths of emission in nm: 373, 404, 432, 461, 500, 353, 593, 634, 665, 693, 728, 761, 801, 835, 874 y 903). For the second part of the system (module 2), the imaging sensor is an InGaAs camera (C10633-13, HAMAMATSU, Japan) with 14 bit depth of digitalization and 340 x 256 pixels of sensing area. This camera uses a short-wave infrared (SWIR) lens (LM12HC-SW 12.5 mm f/#1.4, KOWA, Japan) with improved transmittance between 800nm and 2000 nm. The spectral illumination for this part of the SWIR spectral region is obtained with 7 different groups of LEDs (peak wavelengths of emission in nm: 955, 1071, 1202, 1297, 1451, 1540 y 1630). In total the system provides 23 spectral channels given by LED illumination. The spectral channels provided by the illumination sources have full width at half maximum (FWHM) that ranges from 9.5 to 45 nm in module 1, and between 51 to 126 nm in module 2. The separations between emission peaks in module 1 are around 40 nm, while in module 2 they are above 90nm. This wider separation between peaks of emission in the SWIR spectral region is caused by a more limited commercial availability for the LEDs in this wavelength range.

The two LED sources in the system provide a rather uniform illumination over the sample in an area of 25 x 25 cm^2. For this purpose each specific wavelength of illumination is generated by 4 LEDs arranged in a symmetrical way over a circular ring, with a separation of 90 degrees between them (Fig. 1). In addition, the illumination source includes a diffusing filter in front of the LED elements in order to diminish the influence of their typical directional emission. This configuration allowed us to put the correspondent camera to measure through the hole of the ring like light source and capture the spectral images, thus using diffuse illumination and observation at 0 degrees (d/0º).
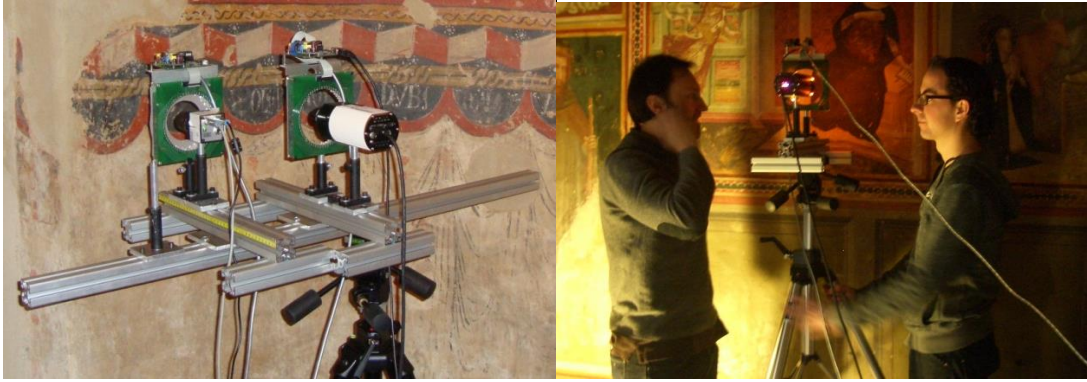
Figure 1. Experimental setup of the portable multispectral system.

The system is mounted on a rail that is assembled to a tripod (Fig. 1), in a way that the system can be displaced laterally over the rail and vertically changing the tripod height. Although, artwork studies are the first intended application of the system, it can be easily adapted to other ones.

IMAGING PROCEDURE, SPECTRAL RECOVERY AND PERFORMANCE EVALUATION

A customized computational interface serves to control all the parameters of the system, synchronization of image acquisition and LED illumination, and implements algorithms for noise correction, calibration and processing of acquired information. The protocol to acquire the spectral image cubes involves the sequential illumination of the field of view with the LED sources and the correspondent acquisition of 23 spectral images. Each image of the cube is the result of averaging 10 frames in order to control the influence of temporal sources of noise, i.e. of the illumination and the sensors.

We corrected the spatial non-uniformity for both, the response of the pixels of the camera and the illumination through a flat fielding process proposed by de Lasarte et.al. [25] based on capturing images of dark frames and of a calibrated white standard panel (BN-R98-SQ12 - 98% reflective, Gigahertz-Optik, Germany). The dark and white standard images are captured under specific camera parameters of offset, gain and exposure time for each channel, which are also later used to collect the images from the samples. The FOV of the system is also referenced to the dimensions of the white standard, i.e. 25x25cm^2 that gives a good compromise considering spatial resolution, working distance and exposure times.

To recover spectral information several procedures can be employed. We used two widely known methods. The first one is the interpolation by splines [26,27] that gives direct access to the spectrum of reflectance. The interpolation methods operates over the digital values in each spectral image (after proper calibration with a standard white or a standard sample with known reflectance) taking them as elements of a reflectance factor image, i. e. as samples of the reflectance spectrum at the wavelength of the spectral channel. The accuracy of the interpolation methods is greatly dependent on the number of channels in the system. In our case spline interpolation gives coarse, but useful, spectral information without the necessity of knowing all system characteristics or prior knowledge of the samples to be imaged. Among all

the interpolation techniques, the spline interpolation was selected because of its characteristic smoothness that fits with the expected type of spectral functions for real materials.

As a second method of spectral reconstruction we implemented the pseudo-inverse method with training [14,28]. This estimation method provides spectral reflectances from digital camera responses through a mapping matrix. This mapping matrix implies a pseudo-inverse procedure minimizing the least-square-error for the training data set of known reflectances and correspondent camera responses. This method gives good spectral results, but it deeply depends on how close is the set of training samples to the samples to capture.

To compare and evaluate the performance in spectral reconstruction of the system we used three different metrics. Two metrics served to compare the estimated spectral curves with respect to the reference spectra: The root mean square error (RMSE) [14,29] that is a widely used metric for spectral evaluation; and the goodness-of-fit coefficient (GFC) proposed by Hernandez-Andrés et.al [29,30]. This GFC is described by equation (1).

$$\text{GFC} = \frac{\left| \sum_j r_o\left(\lambda_j\right) r\left(\lambda_j\right) \right|}{\left\{ \sum_j \left[r_o\left(\lambda_j\right) \right]^2 \sum_j \left[r\left(\lambda_j\right) \right]^2 \right\}^{1/2}}, \tag{1}$$

where $r_o(\lambda_j)$ is the original spectral data at the wavelength λ_j and $r(\lambda_j)$ is the estimated spectrum at the wavelength λ_j. GFC ≥ 0.995, GFC ≥ 0.999 and GFC ≥0.9999 are required for respectively acceptable, good and excellent matches. The third metric is the CIEDE2000 formula (DE00) [31–33] used over the reconstructions in the visible range as a colorimetric evaluation. To compute the color data we used the CIE D65 illuminant and CIE 1964 10° standard observer discretized at 5 nm wavelength intervals.

RESULTS OF ARTWORK IMAGING

We captured images using the multispectral system at the Royal Monastery of Saint Mary of Pedralbes, Barcelona (http://www.bcn.cat/monestirpedralbes/es/). The images were acquired from the wallpaintings located in Saint Michel's chapel that are attributed to the painter Ferrer Bassa. These wallpaintings are an exceptional masterpiece of the Catalan Gothic painting scene dating from the 14th century. Other artwork we imaged was the diptych La Virgen de la Leche (Anonymous) c. 1500. This is oil on wood painting with dimensions around 60 x 40 cm^2.

IMAGING OF WALLPAINTINGS

Fig. 2 contains the RGB and the 23 spectral images captured with the multispectral system for one section of the frescos in Saint Michel's chapel (the RGB image is the combination of the spectral images of 634 nm, 535 nm and 461 nm for the R, G and B channels, respectively). This set of images is an example of the captured information per each section of the mural. By examining the images, conservators and restorers can address features that are hidden in regular trichromatic imaging. As an example of the possibilities offered by the multispectral system, the hexagons in the images of Fig. 2 have uniform color (aside from the scratches and degradation from aging) in the spectral channels of the visible range. Therefore, it is plausible

to think that they should have been painted with the same material, and so they should have the same behavior over the whole spectral range covered by the multispectral system. But, as it is evident from the spectral channels in the infrared, these zones have a part that differs from the rest. It is likely that a retouch has been applied in this part, although using a different material from the original one.

Figure 2. RGB image and the 23 spectral images for a specific zone of the frescos in Saint Michel's chapel at the Royal Monastery of Pedralbes (Ferrer Bassa).

Fig. 3 shows a detail of the image with the possible restoration and the correspondent zone of retouching that has been extracted from the IR information. It has been enhanced and segmented by a thresholding process over the images to help restorers in their regular tasks.

Figure 3. RGB image, spectral image corresponding to 1202nm and a detail with the segmentation of the retouching.

Fig. 4 shows the images for another part of the fresco paintings in Saint Michel's cell and again they allow further insight in the characteristics of the painting. In this case, the spectral images show some strokes in the longer wavelengths in a clearer way than in the visible wavelengths of the range of the images, which suffer more from blackening due to aging and dirt. This kind of findings may be of interest for the study of the aging in the colors of the painting, or of the details of the original image and techniques used by the painter, among other uses the people from the cultural heritage field can give them.
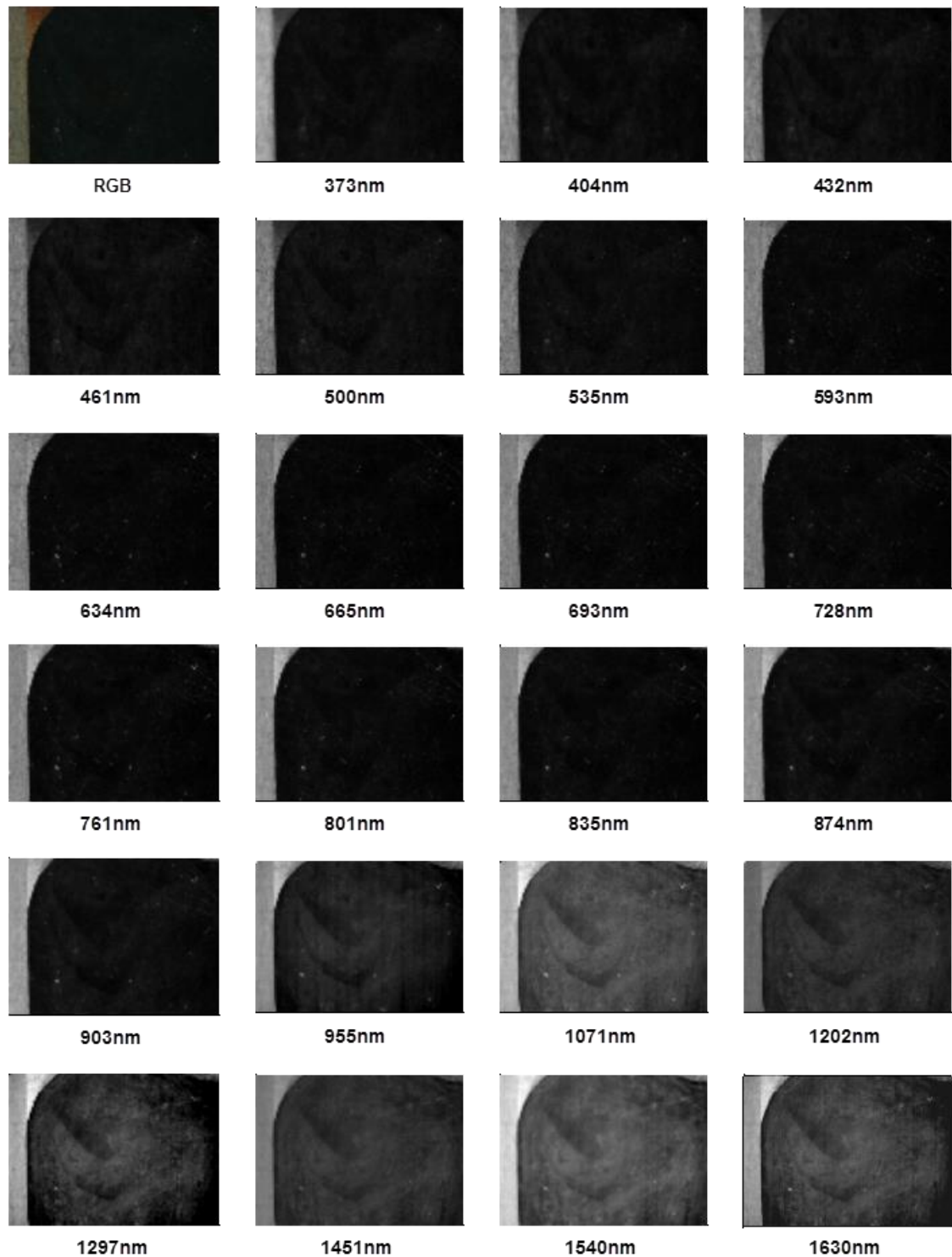
Figure 4. RGB image and the 23 spectral images for a specific zone of the frescos in Saint Michel's chapel at the Royal Monastery of Pedralbes (Ferrer Bassa).

Additionally, spectral and accurate color information can be accessed from the spectral images by using interpolation or estimation methods. In order to access to this information using the pseudo-inverse method, which needs a priori knowledge of spectral samples which are going to be measured, we have used two training sets. One set was a palette of 32 patches generated using the fresco technique and pigments regularly encountered in this kind of wall paintings. These pigments correspond to colors like venetian red, red earth, green earth, burnt

umber (brown), indigo, yellow, yellow ochre, vegetal black among others (Fig. 5 and Fig. 6). For the second training set we measured the spectral reflectance of 22 points over the frescos in Saint Michel's cell with a commercial spectrometer (Spectro 320 R5, Instruments Systems, Germany).This set is also used in this study as the test set for the performance evaluation of the system.
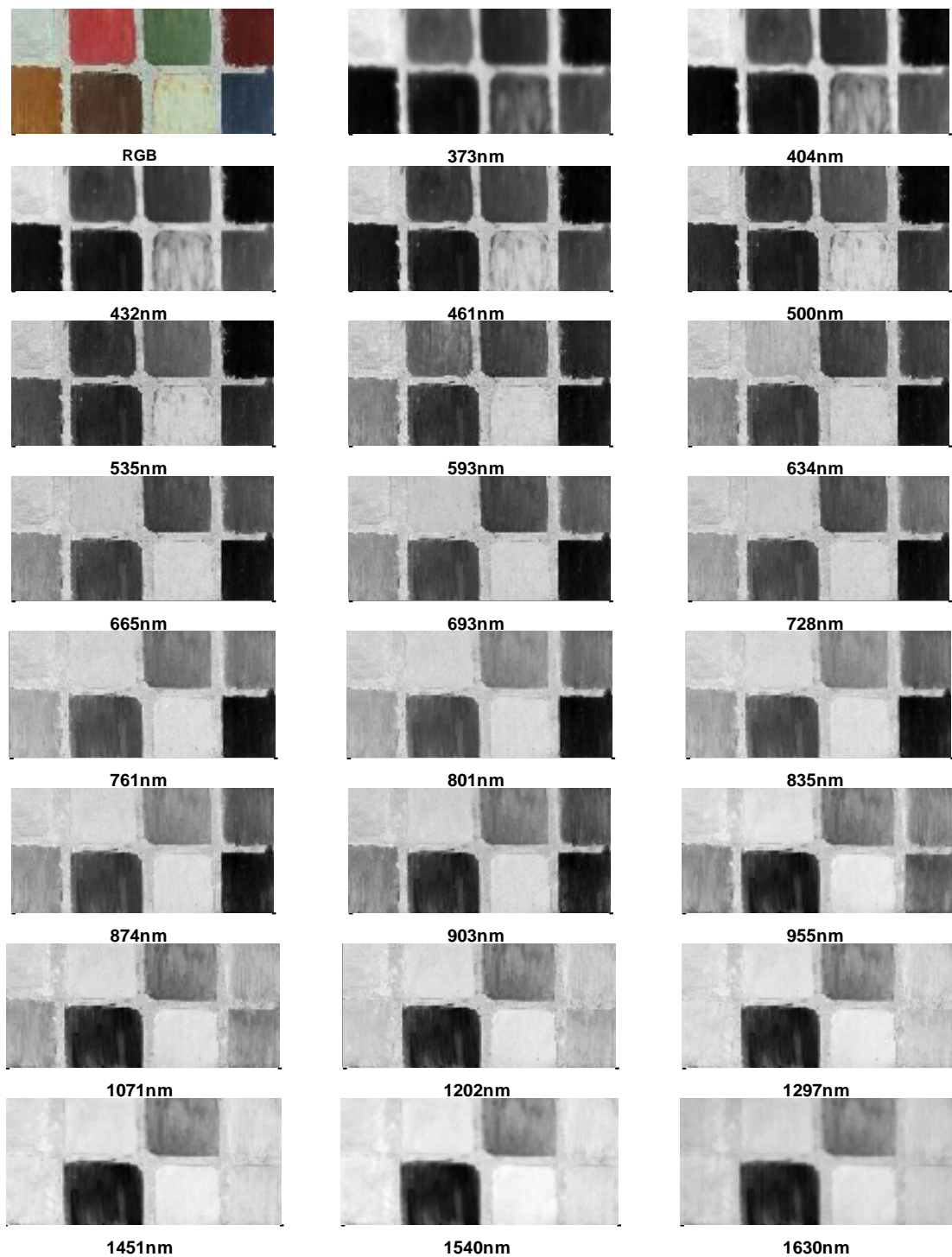

Figure 5. One part of the palette of colored patches (8) using pigments regularly encountered in fresco paintings.

The patches in Fig. 5 are a part of the complete set of pigments prepared as one of the training sets. Their correspondent spectra are depicted in Fig. 6 with the star symbols over their curves, along with the curves for the rest of the training samples belonging to this set. For example, following the burnt umber pigment patch (second row, second column) that is dark in all the spectral images, it can be correlated with its correspondent spectral curve in Fig. 6, the black stared curve.
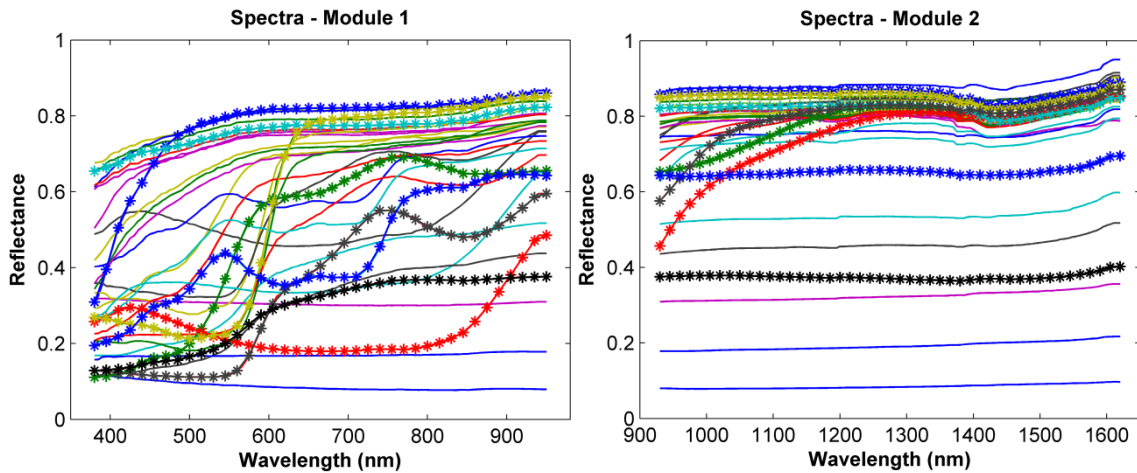

Figure 6. Spectral reflectances from the palette of 32 patches for the training set generated using typical artwork pigments. Measurements carried out with commercial spectrometer (Spectro 320 R5, Instruments Systems, Germany). The lines with stars symbols correspond to the subset of patches shown in Fig. 5.

Table 1 shows the results of performance evaluation in spectral reconstruction for the sample points over the frescos in Saint Michel's cell. From this table it can be observed that the pseudo-inverse method with the sample points as training and test sets presents the best results. In this case it is reasonable to think that some overfitting has taken place. The results for the other two cases, the spline interpolation method and the pseudo-inverse method but using the palette of fresco patches as training set, are still good. Although, with the spline interpolation method having slightly better values, fact that may be related with the rather low variability of the spectral reflectances of the samples, and consequently the more simple fitting between the reference and interpolated spectral curves. Furthermore, in the case of the pseudo-inverse method, it can be influenced by the palette of pigments of the training set. The color differences under 2.5 units represent a rather good colorimetric reconstruction in any of the cases, as well as the values of the RMSE and GFC represent a good spectral fitting in the module 1. A general fact can be drawn from these results, for any of these three cases when the RMSE values are analyzed, is that module 2 presents a poorer performance than module 1. This is due to the lower number of spectral channels in this range.

Table 1. Results of evaluation metrics in spectral estimation for the set of selected sample points (22) over the frescos in Saint Michel's cell (Interp: Spline Interpolation; PSE: pseudo-inverse; TrS: Training Set)

Mean Values	Module 1			Module 2	
	CIEDE2000	RMSE	GFC	RMSE	GFC

Interp	2.08	1.31	0.9995	2.60	0.9996
PSE (TrS: Pigments)	2.43	2.99	0.9987	4.90	0.9991
PSE (TrS: Wall points)	0.69	0.52	0.9999	2.51	0.9998

IMAGE COMPOSITION OF LARGE SIZE PIECES

Another challenge typically found in artwork imaging is the capture of large size images, like is the common case in frescos and other formats of paintings. Fig. 7 shows the result of an image composition for the painting La Virgen de la Leche. This image has been captured with the multispectral system by a sequence of movements and posteriorly assembled from the set of sub-images using a stitching algorithm implemented in Matlab platform based on computing correlations of intersecting zones of individual images.

Figure 7. Result of the image composition for the painting La Virgen de la Leche from a set of sub-images acquired using the multispectral system (Painting from the collection of the Royal Monastery of Pedralbes).

The painting in Fig. 7 shows some deterioration, like the vertical crack in the middle of the painting or the color degradation on the background. In these situations the restorers and museum workers can take advantage of the detailed spatial information provided by the composed images of the system to assess the process over time or to study in more detail a course of action, if it is required. For example the Fig. 8 shows three images where with a histogram equalization to the image corresponding to the spectral channel of 1202 nm (Fig. 8c) is enough to enhance and visualize the underling layers where cracking of the materials can be observed. Additionally, as shown before, other possible details from restorations are also revealed, highlighted in Fig. 8c, which are not visible in the RGB image or the 590 nm spectral channel.
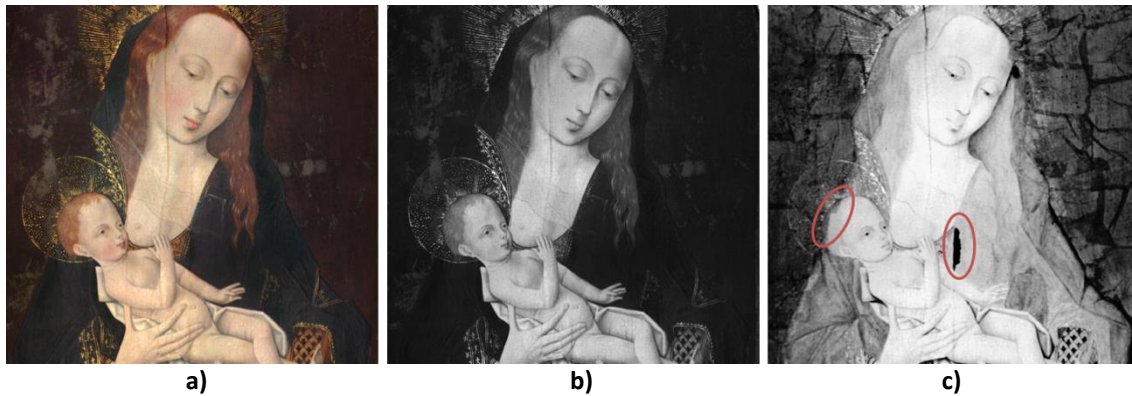
Figure 8. Comparison of a portion of the painting La Virgen de la Leche to show the cracking of underling layers of the painting. Shown a) RGB image, b) Spectral channel of 590 nm, and c) Spectral channel of 1202 nm enhanced through histogram equalization.

CONCLUSIONS

The information provided by the LED based system that has been presented in this work showed that it could be a useful tool in environments involving cultural heritage studies and artwork conservation. Various examples of features in the artworks that were hidden to plain sight or trichromatic imaging were revealed when using the system, showing the offered possibilities by the system which can overcome some of the limitations of current techniques commonly employed in this field. The evaluation in spectral and colorimetric performance also showed that the system is a reliable tool for providing pixel-wise reflectance information over a wide range of the spectrum. The composition of a large size artwork from a set of sub-images was successfully achieved showing the versatility of the system and suitability for its use in this kind of painting formats.

This kind of multispectral systems using LED technology offer a cost effective option with good characteristics of portability, compactness, modularity and reliability that we think are also susceptible of being exploited in other areas of application. Additionally, it is easy to combine or modify the basic setup of the system implemented in this work with wide range of other elements to expand the possibilities of the system, for example, like filters for offering capabilities of luminescence evaluation.

ACKNOWLEDGEMENTS

REFERENCES

1.	T. G. Giallorenzi, "Optical technology in naval applications," Opt. Photonics News **11**, 24 (2000).

2.	Q. Weng, ed., *Advances in Environmental Remote Sensing: Sensors, Algorithms, and Applications* (CRC Press, 2011), p. 610.

3. N. L. Everdell, I. B. Styles, A. S. Calcagni, J. Gibson, J. C. Hebden, and E. Claridge, "Multispectral imaging of the ocular fundus using light emitting diode illumination.," Rev. Sci. Instrum. **81**, 093706 (2010).

4. M. Vilaseca, R. Mercadal, J. Pujol, M. Arjona, M. de Lasarte, R. Huertas, M. Melgosa, and F. H. Imai, "Characterization of the human iris spectral reflectance with a multispectral imaging system.," Appl. Opt. **47**, 5622–5630 (2008).

5. D. F. Barbin, G. ElMasry, D.-W. Sun, and P. Allen, "Predicting quality and sensory attributes of pork using near-infrared hyperspectral imaging.," Anal. Chim. Acta **719**, 30–42 (2012).

6. X. L. Wang, B. Waske, and J. Benediktsson, "Ensemble methods for spectral-spatial classification of urban hyperspectral data," in *Geoscience and Remote Sensing Symposium, 2009 IEEE International, IGARSS 2009* (IEEE, 2009), Vol. 4, pp. IV–944.

7. R. Lu and Y. Peng, "Development of a multispectral imaging prototype for real-time detection of apple fruit firmness," Opt. Eng. **46**, 123201 (2007).

8. M. Barni, A. Pelagotti, and A. Piva, "Image processing for the analysis and conservation of paintings: opportunities and challenges," IEEE Signal Process. Mag. **22**, 141–144 (2005).

9. J. Y. Hardeberg, F. Schmitt, H. Brettel, J. P. Crettez, H. Maitre, and Henri Maitre, "Multispectral image acquisition and simulation of illuminant changes," Colour imaging Vis. Technol. 145–164 (1999).

10. J. Redman, "Advances in Digital Imaging for Fine Art and Cultural Heritage," in *NIP23 and Digital Fabrication* (2007), pp. 355–363.

11. J. K. Delaney, J. G. Zeibel, M. Thoury, R. Littleton, M. Palmer, K. M. Morales, E. R. de la Rie, and A. Hoenigswald, "Visible and infrared imaging spectroscopy of Picasso's Harlequin musician: mapping and identification of artist materials in situ.," Appl. Spectrosc. **64**, 584–94 (2010).

12. C. Daffara, E. Pampaloni, L. Pezzati, M. Barucci, and R. Fontana, "Scanning multispectral IR reflectography SMIRR: an advanced tool for art diagnostics.," Acc. Chem. Res. **43**, 847–856 (2010).

13. C. Bonifazzi, P. Carcagnì, R. Fontana, M. Greco, M. Mastroianni, M. Materazzi, E. Pampaloni, L. Pezzati, and D. Bencini, "A scanning device for VIS–NIR multispectral imaging of paintings," J. Opt. A Pure Appl. Opt. **10**, 064011 (2008).

14. M. Vilaseca, J. Pujol, M. Arjona, and M. de Lasarte, "Multispectral system for reflectance reconstruction in the near-infrared region," Appl. Opt. **45**, 4241–4253 (2006).

15. L. Kong, D. Yi, S. Sprigle, F. Wang, C. Wang, F. Liu, A. Adibi, and R. Tummala, "Single sensor that outputs narrowband multispectral images.," J. Biomed. Opt. **15**, 10502 (2010).

16. S. Mathews, "Design and fabrication of a low-cost, multispectral imaging system.," Appl. Opt. **47**, F71–6 (2008).

17. A. Basiri, M. Nabili, S. Mathews, A. Libin, S. Groah, H. J. Noordmans, and J. C. Ramella-Roman, "Use of a multi-spectral camera in the characterization of skin wounds," Opt. Express **18**, 3244 (2010).

18. J. Y. Hardeberg, F. Schmitt, and H. Brettel, "Multispectral color image capture using a liquid crystal tunable filter," Opt. Eng. **41**, 2532 (2002).

19. C. D. Tran, "Principles, Instrumentation, and Applications of Infrared Multispectral Imaging, An Overview," Anal. Lett. **38**, 735–752 (2005).

20. M. B. Bouchard, B. R. Chen, S. Burgess, and E. M. C. Hillman, "Ultra-fast multispectral optical imaging of cortical oxygenation, blood flow, and intracellular calcium dynamics.," Opt. Express **17**, 15670–15678 (2009).

21. L. Fauch, E. Nippolainen, and A. a. Kamshilin, "Accuracy of the reflectance spectrum recovery in a light-emitting diode-based multispectral imaging system," Opt. Eng. **51**, 053201 (2012).

22. J. Li and R. K. Y. Chan, "Toward a UV-visible-near-infrared hyperspectral imaging platform for fast multiplex reflection spectroscopy.," Opt. Lett. **35**, 3330–2 (2010).

23. M. Brydegaard, A. Merdasa, H. Jayaweera, J. Ålebring, and S. Svanberg, "Versatile multispectral microscope based on light emitting diodes.," Rev. Sci. Instrum. **82**, 123106 (2011).

24. A. Paviotti, F. Ratti, L. Poletto, and G. M. Cortelazzo, "Multispectral Acquisition of Large-Sized Pictorial Surfaces," EURASIP J. Image Video Process. **2009**, 1–17 (2009).

25. M. de Lasarte, J. Pujol, M. Arjona, and M. Vilaseca, "Optimized algorithm for the spatial nonuniformity correction of an imaging system based on a charge-coupled device color camera.," Appl. Opt. **46**, 167–174 (2007).

26. H. Andrews, "Cubic splines for image interpolation and digital filtering," IEEE Trans. Acoust. **26**, 508–517 (1978).

27. J. Kiusalaas, *Numerical Methods in Engineering with MATLAB ®* (Cambridge University Press, 2005).

28. H.-L. Shen, P.-Q. Cai, S.-J. Shao, and J. H. Xin, "Reflectance reconstruction for multispectral imaging by adaptive Wiener estimation," Opt. Express **15**, 15545 (2007).

29. F. H. Imai, M. R. Rosen, and R. S. Berns, "Comparative study of metrics for spectral match quality," in *Proceedings of the First European Conference on Colour in Graphics, Imaging and Vision* (2002), pp. 492–496.

30. J. Hernández-Andrés, J. Romero, and R. L. Lee, "Colorimetric and spectroradiometric characteristics of narrow-field-of-view clear skylight in Granada, Spain.," J. Opt. Soc. Am. A. Opt. Image Sci. Vis. **18**, 412–420 (2001).

31. M. Melgosa, A. Trémeau, and G. Cui, "Colour Difference Evaluation," in *Advanced Color Image Processing and Analysis*, C. Fernandez-Maloigne, ed. (Springer New York, 2013), pp. 65–85.

32. G. Sharma, W. Wu, and E. N. Dalal, "The CIEDE2000 color-difference formula: Implementation notes, supplementary test data, and mathematical observations," Color Res. Appl. **30**, 21–30 (2005).

33. M. R. Luo, G. Cui, and B. Rigg, "The development of the CIE 2000 colour-difference formula: CIEDE2000," Color Res. Appl. **26**, 340–350 (2001).